Analyst

Accepted Manuscript

This article can be cited before page numbers have been issued, to do this please use: M. Muppidathi, P. Perumal, R. Ayyanu and S. Subramanian, *Analyst*, 2019, DOI: 10.1039/C9AN00139E.

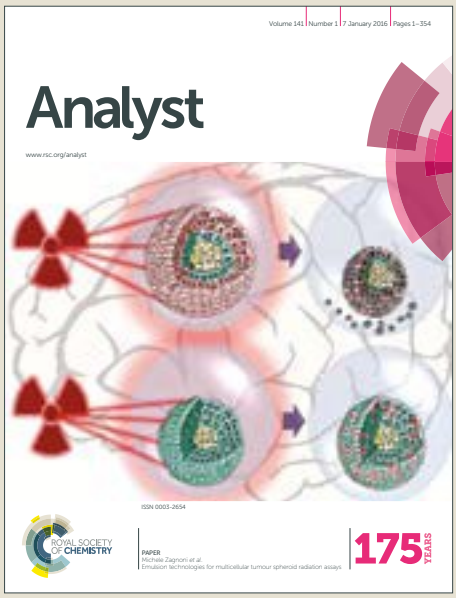

View Article Online
DOI: 10.1039/C9AN00139E

Immobilization of ssDNA displacement from Metal-Organic Framework derived magnetic porous carbon (MPC) composite based fluorescent sensing platform for detection of arsenate ions

Muppidathi Marieeswaran[a], Perumal Panneerselvam[a]*, Ayyanu Ravikumar[a], Subramanian Sivanesan[b]

a* Department of Chemistry, SRM Institute of Science and Technology, Kattankulathur

603 203, Tamil Nadu, India

b Department of Applied Science and Technology, A.C. Tech, Anna University, Chennai,

600 025, India

* Corresponding author & E-mail address: panneerselvam.pe@ktr.srmuniv.ac.in

panneerchem82@gmail.com; Tel: +91 9688538842

View Article Online
DOI: 10.1039/C9AN00139E

Abstract

In this work, we fabricated Metal-Organic Framework derived magnetic porous carbon (MPC) composite using a one-pot solid state template method, the synthesized composite were confirmed with various spectroscopic techniques and proved that composite having effectively quenching of ssDNA. This properties was essentially utilizes with specifically and efficient recognition harmful arsenate ions. The FAM-labeled single strand DNA (FAM-ssDNA) adsorbed on the surface of MPC composites and formation of immobilization ssDNA via π-π stacking interaction, which results the fluorescence emission intensity was quenched. The fluorescence quenching efficiency was achieved 96% due to huge surface area of MPC composites. Upon the addition of As (V) ions into our sensing system, its fluorescence emission dramatically increased appropriate strong affinity of As (V) on the surface of MPC composites. Consequently, the adsorbed FAM-ssDNA was spontaneously displaced from the surface of MPC composite, and then fluorescence intensity was retained. Based on this mechanism, the fabricated biosensor exhibited highly sensitive and good fluorescence response to As (V) the detection limit as low 630 pM at the range from 0 to 15 nM. Furthermore, the sensing system suitable for diverse biological and environmental samples.

Keywords: MPC composites, Immobilization ssDNA, FRET, Arsenate ions

View Article Online
DOI: 10.1039/C9AN00139E

1. INTRODUCTION

Heavy metal contamination is a serious hazardous to human health and the environment. Among several heavy metal ions, including the inorganic form of arsenic was exceedingly contaminated to environmental soil and aquatic system, its cause numerous dangerous effects to human organs and eco-system. In common, arsenic was existed two different variable oxidation states, namely arsenite (III) & arsenate (IV). The As (III &V) exposure has serious health effects leads to cancer, heart disease, diabetes and even death [1-6]. Harmful nature of arsenite (III) and arsenate (IV) is essential for detoxification to allowed limits. World Health Organization (WHO) and U.S. Environmental Protection Agency (EPA) had predetermined that the maximum allowed concentration of arsenate from 10 to 50 nM [7, 8]. Up to date, most of the researchers have been focused on detection of As (V) and more challenge to detection of As (V) [9-12]. The defined methods are existed methods namely adsorption and oxidation. The adsorption methods existing for monitoring of As (III and V) ions such as atomic absorption and emission spectroscopy, inductively coupled plasma spectrometer, surface-enhanced Raman scattering, and oxidation As (III) to As (V) [13-17]. However, defined methods were limitation to apply, because of rigid sample preparation, pre-concentration procedures, time-consuming, sophisticated instruments and professional personnel. Currently, developed methods are colorimetric, fluorescence and electrochemical sensors for detection of As (V) [18-22]. Among them, fluorescence methods gain great attention for detection of As (V) due facile operating process, sensitive, selective and easily applicable for real sample analysis.

Owing to unique characteristics of nanomaterials have been attracted great attentions for biosensor applications due to the high surface area and high quenching efficiency. The Fe_3O_4 nanoparticles with appropriate surface chemistry can be used for versatile applications such as

View Article Online
DOI: 10.1039/C9AN00139E

biosensor, drug delivery, and cell separation [23]. The Fe_3O_4 nanoparticles have been attracted tremendous attention for its magnetic and adsorption properties. DNA probes are highly adsorbed on the surface Fe_3O_4 NPs via phosphate backbone [24] and As (V) also high adsorption affinity of Fe_3O_4 NPs. The adsorption properties of Fe_3O_4 NPs were used for the detection of As (V) based on the displacement of adsorbed DNA probes [25,26]. Therefore, the Fe_3O_4 NPs was better candidate for detection of As (V) but limits by some drawbacks such as less surface areas, large grain boundaries, easy aggregation, and low stability. Overcome these drawbacks, Metal-Organic frameworks gain considerable attention to scientific communities due to porous materials with attractive physiochemical properties such as high surface area, tunable architecture and tunable pore structure. MOFs with great potential applications in a versatile file such as gas separation and storage, adsorption, optical electronics materials, catalysis, drug delivery, photocatalysis sensor applications [27-29]. Interestingly, metal-organic frameworks template method facile to fabricated metal oxide with different shapes and fascinating properties. This method effectively prevented metal-oxide aggregation of Fe_3O_4 nanoparticles, suitable organic linker also act as reducing agent and further transform to porous into frameworks. These properties more effectively applicable for sensing application [30-35]. The MPC composites having fascinating properties such as quenching materials as well as adsorption and stability. Li Wang.et.al reported by metal oxides/carbon nanocomposites [36].

In this study, we successfully developed a fabricated Metal-Organic Framework derived magnetic porous carbon (MPC) composite for fluorescent biosensor using a one-spot solid-template method. The functionalized material acts as high performance and a novel application of the fluorescent sensing platform for highly sensitive detection of arsenate ions. It was found that the MPC composites bind with FAM-ssDNA, which results the fluorescence intensity was

View Article Online
DOI: 10.1039/C9AN00139E

drastically quenched due to MPC/FAM-ssDNA complex. Subsequently, introduced of As (V) into sensing system the fluorescence intensity is enhanced. Because of the arsenate ions binding with a surface of MPC composites and immobilization DNA was displacement from the surface of the MPC composites. The result demonstrates that the proposed sensor can achieve highly sensitive and selective towards As(V), with a detection limit 3nm. In addition, the main advantage of our sensing system formation of MPC-As(V) is easily separated. Therefore, "turn-off" and "on" fluorescence sensing scenario with highly efficient and effective detection of As (V) was successfully achieved.

2. Experimental section

2.1. Chemical and characterization

All chemical purchased from Sigma Aldrich, Avra and SRL chemicals in analytical grade, solvent were used without further any purification. Ferric nitrate ($Fe(NO_3)_3.6H_2O$), fumaric acid, Dimethylformamide (DMF), methanol, mercury nitrate, cadmium chloride, Ferric chloride, magnesium chloride, silver chloride and other standard . All the reagents were prepared from Milli-Q water. The buffer prepared from 50 mM Tris-HCl buffer, NaCl (50 mM) and $MgCl_2$ (5 mM) (pH= 7.4). The stock solution of DNAs was prepared by using a Tris-HCl buffer. The synthesized DNA were purchased from integrated DNA (IDT, Avantor, India) technologies

DNA probe sequence: 5'-FAM-ATCCTCTCTCAAAAACAACACAACAAAC-3'

The Fluorescence spectra analysis on Jasco FP-8300 spectrofluorometer using cuvettes of 1.0 cm path length with a xenon lamp excitation source with an excitation wavelength of 490 nm. The morphology and crystalline structure information of MPC composites were evaluated using scanning electron microscopy (SEM, FEI Quanta FEG 200) and high-resolution

View Article Online
DOI: 10.1039/C9AN00139E

transmission electron microscopy (HRTEM, JEOL, JEM, Fb-2000) and. The X-ray diffraction spectrum is performed on the PAN analytical X'pert pro X-ray diffractometer with CuKα radiation. The bonding information studies were used Agilent Technologies FTIR spectrometer (USA) is used to record the Fourier transform infrared (FT-IR) spectra with the ATR mode. Raman spectra (HORIBA France, LABRAM HR Evolution) were recorded.

2.2. Synthesis of metal-Organic framework derived magnetic porous carbon (MPC) composites

The MPC composite was prepared according to the improved procedure [37]. In a typical synthesis, (1 mmol) $FeCl_3.6H_2O$, (1 mmol) fumaric acid were dissolved in 25 mL Mili-Q water and stirred for 30 mins to form a homogeneous solution. Subsequently, the above mixture was transferred into a 100 mL crow-capped tube and held to at 100^{o}C for 4 h. The resulting product was washed with water and ethanol repeatedly, and drying in hot air oven at 60^{o}C overnight. Finally, the brown colored product was collected MOF (Fe-MIL-88A) and direct pyrolysis at 600^{o}C under inert atmosphere condition for 4h then cooling to room temperature and finally collected black colored MPC composites.

2.3. Fluorescence detection experiments

In a typical fluorescence detection of As (V), 50 µL of 10 µM FAM- ssDNA and 20 µg/mL of MOF@ Fe_3O_4 composites suspension were mixed with in a 50 mM Tris-HCl buffer solution (pH=7.4) were sequentially after 1 min, the solution was transferred in to cuvette. Subsequently, the freshly prepared 10 µL As (V) ion stock solution was added different concentrations (0 to 15µM) and incubated for 1 min. The fluorescence intensity was measured by excitation at 490 nm and emission was observed at 520 nm respectively.

View Article Online
DOI: 10.1039/C9AN00139E

3. Result and discussion

The structural morphologies of the synthesized MOF and MPC composite were characterized by SEM and TEM analysis and displyed in fig.1a-d. As shown in fig.1a , which clearly reveals that hexagonal micro-spindle rod shape with uniform particle distribustion. In Fig.1b shows that, the Fe_3O_4 nanoparticles randomly dispered on the surface of MOF during the calcination at high temprature (600^{o}C). moreover, the TEM images (Fig.1d) undoubtably indicates hexagonal rod like morphology.The magnified HR-TEM image shows Fe_3O_4 nanoparticles appear over the surface of MOF (fig.2c). From this Fe_3O_4 nanoparticles was prepared by facile methods without aggreation using MOF tempate method.

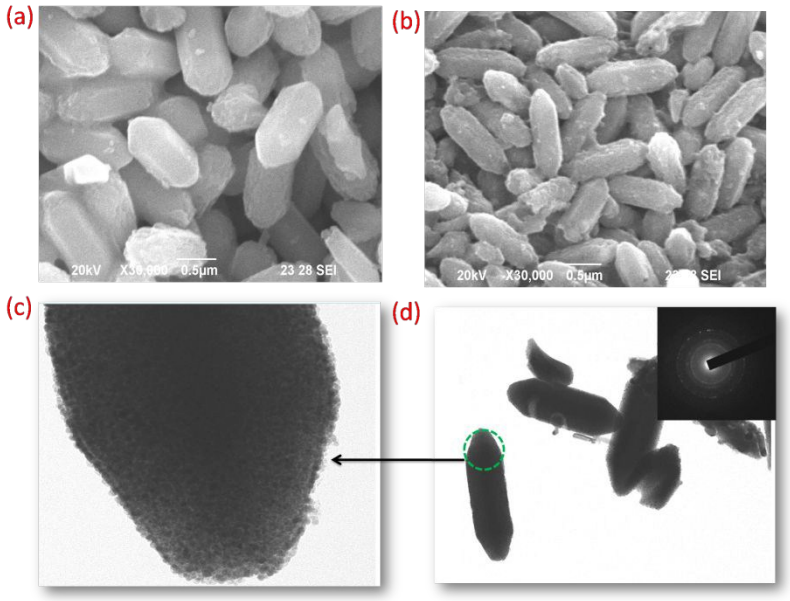

Fig.1. Illustration of SEM images of Fe-MIL-88A (a) and MPC (b). (c & d) TEM images of MPC

The structural information and phase purity to examine the synthesized MOF and MOF@ Fe_3O_4 composites by Powder X-ray diffraction shows in Fig.2. The XRD patterns of MOF features with characteristic diffraction peaks which are perfectly match with previously reported. All the diffraction peaks of MOF disappeared and a new peak appears for MPC composites. The diffraction peaks are 30.3^o, 35.7^o, 43.5^o, 57.37^o and 63^o were indexed as the diffraction of the

View Article Online
DOI: 10.1039/C9AN00139E

crystalline planes is 220, 311, 400, 511, and 440. This observation, strong evidence for the formation of MOF derived magnetic porous carbon composites [32].

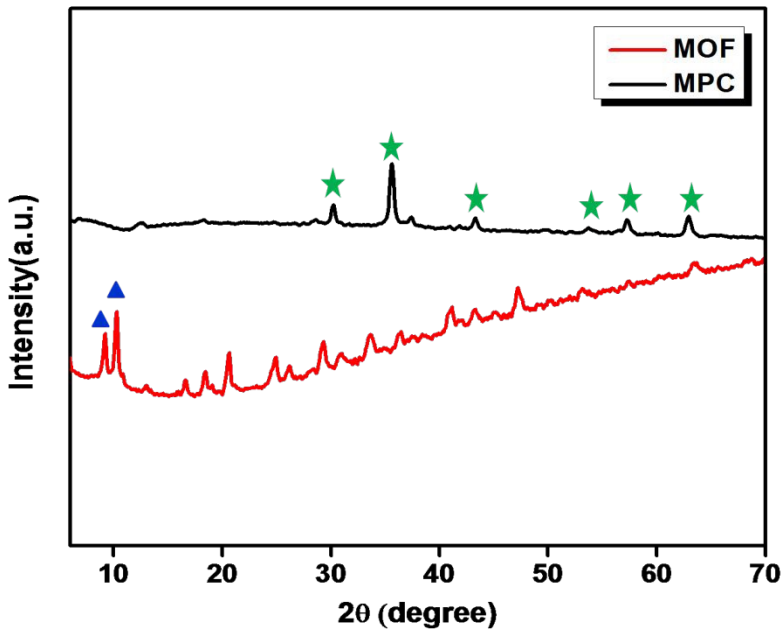

Fig.2 The XRD pattern of MOF and MPC composites

The FT-IR spectra of MOF, and MPC composites depicted in Figure.3a. The precursor fumaric acid and ferric nitrate having carbonyl and free hydroxyl groups are obtain corresponding band as 3510 and 1679 cm^{-1} respectively, which carbonyl group (C=O) shifted to lower band at 1600 cm^{-1} due to formation of MOF through coordination bond with inorganic node. This characteristic peak was confirming that formation MOF (Fe-MIL-88A). After performed in direct pyrolysis of MOF, that having spinel ferrate eascily converted to MPC composite that assigned at 567cm^{-1} attribute to the iron-oxide (Fe-O) in the surface of MPC composites is displayed (Fig.3b).

View Article Online
DOI: 10.1039/C9AN00139E

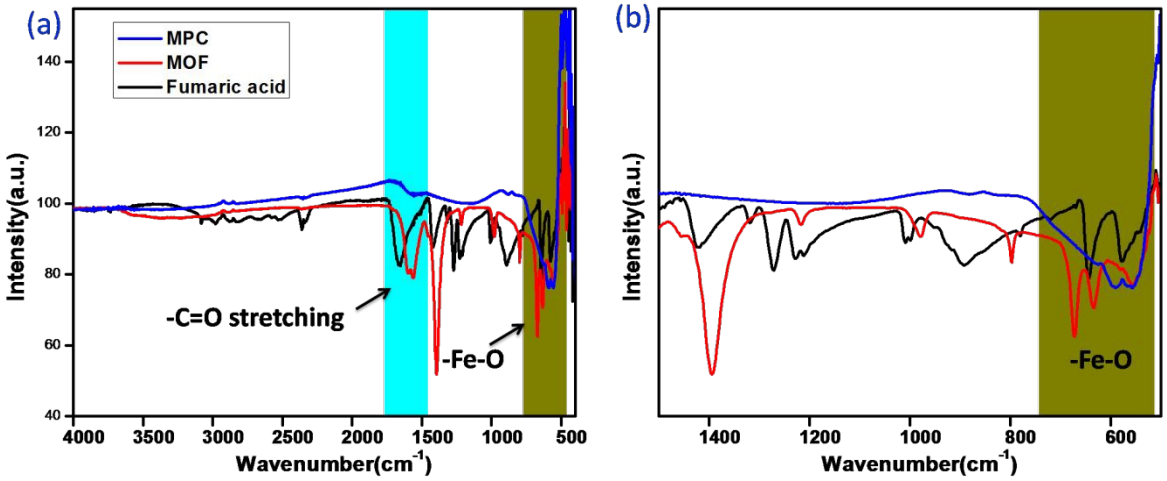

Fig.3 (a) FT-IR spectra of formation of MOF and MPC composites. (b) Enlarged iron- oxide bonding in MPC composites.

In addition, the Raman scattering was performed for fabricated MPC composites were analyzed with excitation of 633nm was depicted in Figure.4. The synthesized MPC composites exhibited two major peaks at 1311cm^{-1} and 1606cm^{-1} and the charactertics peaks represented D and G band respectively. The major band emphasizes regarding deep interaction between MPC composite and ssDNA, which like the graphene-like composites.

View Article Online
DOI: 10.1039/C9AN00139E

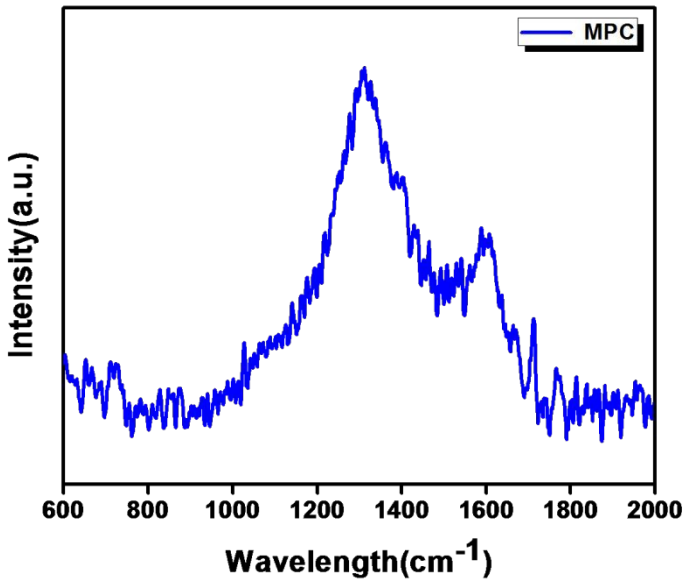

Fig.4. Raman spectra of MPC composites.

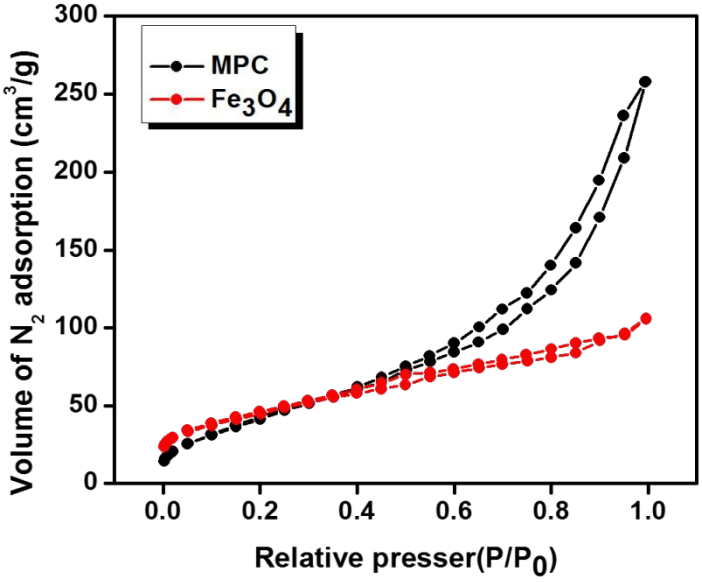

Fig.5. N2 adsorption and desorption isotherms of Fe_3O_4 NPs and MPC composite.

The N_2 adsorption–desorption studies shows the surface area of Fe_3O_4 NPs and MPC composites and results shown in fig.5. As shown in fig.8, the BET surface area and pore volume of pristine Fe_3O_4 NPs and MOF derived magnetic porous carbon (MPC) is found to be 61.218

View Article Online
DOI: 10.1039/C9AN00139E

m^2/g , 136.692 m^2/g and 0.108 cc/g, 0.379 cc/g, respectively. In this observation, MOF derived magnetic porous carbon (MPC) having high surface area and pore volume compared pristine Fe_3O_4 NPs. Which results, the MPC composites attained high adsorption ability of FAM-ssDNA due to high surface area.

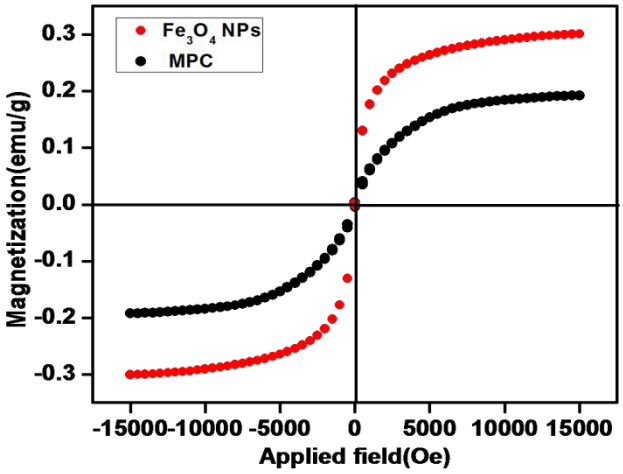

Fig.6. Vibrating Sampling Magnetism analysis of Fe3O4 NPs and MOF derived magnetic porous carbon (MPC).

In this analysis, the pristine Fe_3O_4 NPs have high magnetism when compared to MOF derived magnetic porous carbons (MPC). Eventhough, the MPC have less magnetism it was easily separated by external magnet after the formation of MPC/As(V).

The EDX data for MPC Composite before and after addition of arsenate and SEM mapping of MPC/As(V) displayed in Fig.(S_1&S_2). From the fig.S_1a shows that MPC composite contains Fe, O and C elements. Further addition of arsenate into to MPC composite, the MPC composite having higher affinity towards the arsenate ions. Which results, provide evidence for elements Fe, O, C and As(V) presence in MPC/As(V) and results was displayed in Fig.S_1b. Further SEM-

View Article Online
DOI: 10.1039/C9AN00139E

Elements mapping analysis of MPC/As (V) was done to confirmed the presence of C, O, Fe and As(V) shown in fig.S_2.

3.1 Interaction and quenching mechanism of MPC composites in FAM-ssDNA

The MPC composites have appreciably interacted with FAM attached ssDNA. The fig.5a explain systematically adsorption and desorption will be occurred FAM attached ssDNA with MPC composites. Initially, FAM attached ssDNA and MPC composites mixed well and both interact together with intermolecular force. Notably, MPC composites were behaving like graphene like composites (fig.4). However, two components were having negative surface backbone, which are capable to bind through electrostatic interaction, even not giving importance only negligible quantity. This sensing system giving superior priority to π-π stacking interaction. Moreover, may be hydrogen bonding also supports to increase the quenching effect.

The MPC composites show significantly effect on the fluorescence of FAM-ssDNA and fluorescence quenching mechanism were displayed in (fig.2b). In addition of MPC composites in to the solution of FAM-labeled single stand DNA, which results indicates fluorescence emission intensity was robustly quenched. While using FAM-ssDNA facile to monitored adsorption and recovery via fluorescence properties and high quenching efficiency compared other type of dye labeled ssDNA [38]. Remarkably, MPC composites showed broad absorption spectra at the range of 400-800 nm and the FAM-ssDNA appeared emission peaks at 525 nm in (fig.5b). The absorption and emission spectra overlapping were undoubtedly proved fluorescence resonance energy transfer (FRET) mechanism. On the other hand, quench the fluorophore with help of Photo Electron Transfer (PET) process by Fe_3O_4 NPs. This result reveals that our sensing system is applicable for FRET mechanism and may be PET mechanism [39-43]. The Quenching

View Article Online
DOI: 10.1039/C9AN00139E

efficiency was quantitatively measured this formula QE= $(F_0-F_1/F_0) \times 100\%$, where F_0 was the fluorescence intensity of FAM-ssDNA and F_1 is the fluorescence intensity of attached with of MOF@ Fe_3O_4 composites with FAM-ssDNA. Quenching efficiency was achieved 96% due to energy transfer process respectively.

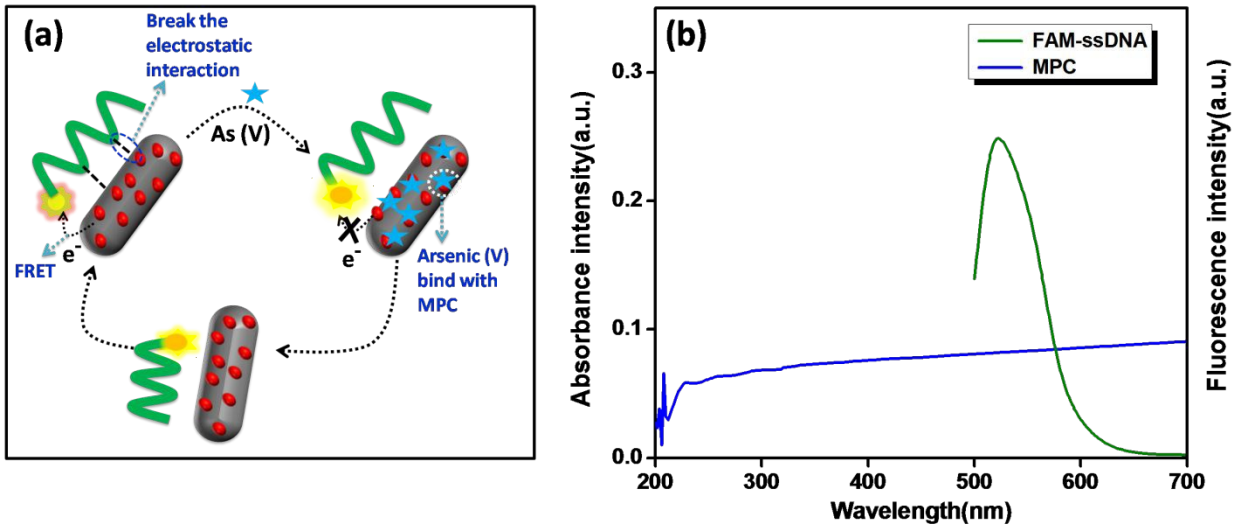

Fig.7 (a) systematically explain adsorption-desorption mechanism between Dye-labeled single strand DNA and MPC composites. (b) Absorption spectra of MPC composites and Emission spectra of between Dye-labeled single strand DNA

3.2 Sensing mechanism

The working principle of this proposed sensing system displayed the scheme.1. In this sensing system using single strand DNA with attached FAM. In the absence of As (V), the FAM labeled single strand DNA is binding with MPC composites via π-π stacking interaction between the surface of MPC composites and nucleobases in ssDNA and fluorescence intensity completely quenched. Upon the addition of As (V) in this sensing system, the As (V) is strongly binding with Fe_3O_4 nanoparticles on the surface of MPC composites. At the same time, FAM labeled

View Article Online
DOI: 10.1039/C9AN00139E

ssDNA is released from the surface of MPC composites, which results shows fluorescence intensity is enhanced. In addition, the main advantage of this sensing system the formation of MOF@Fe_3O_4/As (V) can separate by super magnet. The displacement of the FAM-ssDNA can undergo adsorbed with MPC composites to displace the FAM ssDNA and addition of As (V), consequently providing the significant fluorescence intensity. Therefore, this sensing system is detecting the very low concentration of As (V) with high sensitivity and selectivity

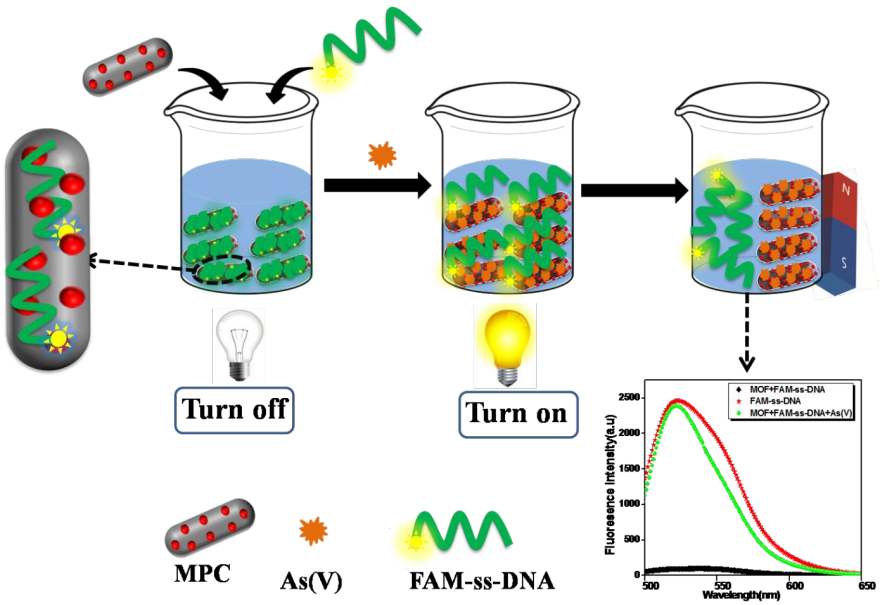

Scheme.1 Schematic representation of sensing mechanism using MPC composites and FAM-ssDNA.

3.4 Detection feasibility

The optical properties were studied by UV-Visible and fluorescence spectroscopy. The UV-Visible spectra of MPC composites showed broad absorption band at 400-700 nm and pristine FAM-ssDNA prominent adsorption peak appeared at 490nm (Figure.6a). Further mixed

View Article Online
DOI: 10.1039/C9AN00139E

with MPC composites, a FAM-ssDNA absorption peak 490nm was disappeared and adsorption band intensity was drastically gone to hypochromic shift due to quenching of the FAM-ssDNA deeper interaction with MPC composites. Moreover, the addition of As(V) into MPC composites and FAM-ssDNA, as result of this sensing system prefer to bind with As(V) and adsorption band were retained to hyperchromic shift at the range of adsorption band is 490 nm. In addition fluorescence responses of this sensing system was investigated (Figure.6b). The free FAM-ssDNA exhibits high fluorescence emission signal (in red line). After subsequent addition of MOF@ Fe_3O_4 composites in the solution containing FAM-ssDNA the fluorescence intensity was decreased due to immobilization of FAM-ssDNA with the surface of MPC composites (in black line). Furthermore, adding arsenate into sensing system the fluorescence intensity retained to original form (in blue line) because of arsenate more affinity to bind MPC composites becomes MPC/As(V) complex. The fluorescence quenching efficiency at optimum amount MPC composites was investigated (Fig.6c). The fluorescence emission intensities of FAM-ssDNA was measured toward the addition of various amount of MPC composites such as 0.1, 0.2, 0.3, 0.4 and 0.5 µg with 20nm of FAM-ssDNA. The fluorescence intensity is decreased after increasing the amount of MPC composites. However, when the amount of MPC composites increasing up to 0.5 µg the fluorescence intensity gets saturated. Therefore, 0.5 µg of MPC composites is used for further experimental conditions. Moreover, to evaluate the quenching efficiency MPC composites and Fe_3O_4 NPs (Fig.6d) in presence of FAM-ssDNA. The fluorescence quenching and recovery efficiency of MPC composites were comparatively higher active than bare Fe_3O_4 NPs. These results revealed that superior detection of As (V) using FAM-ssDNA with MPC composites.

View Article Online
DOI: 10.1039/C9AN00139E

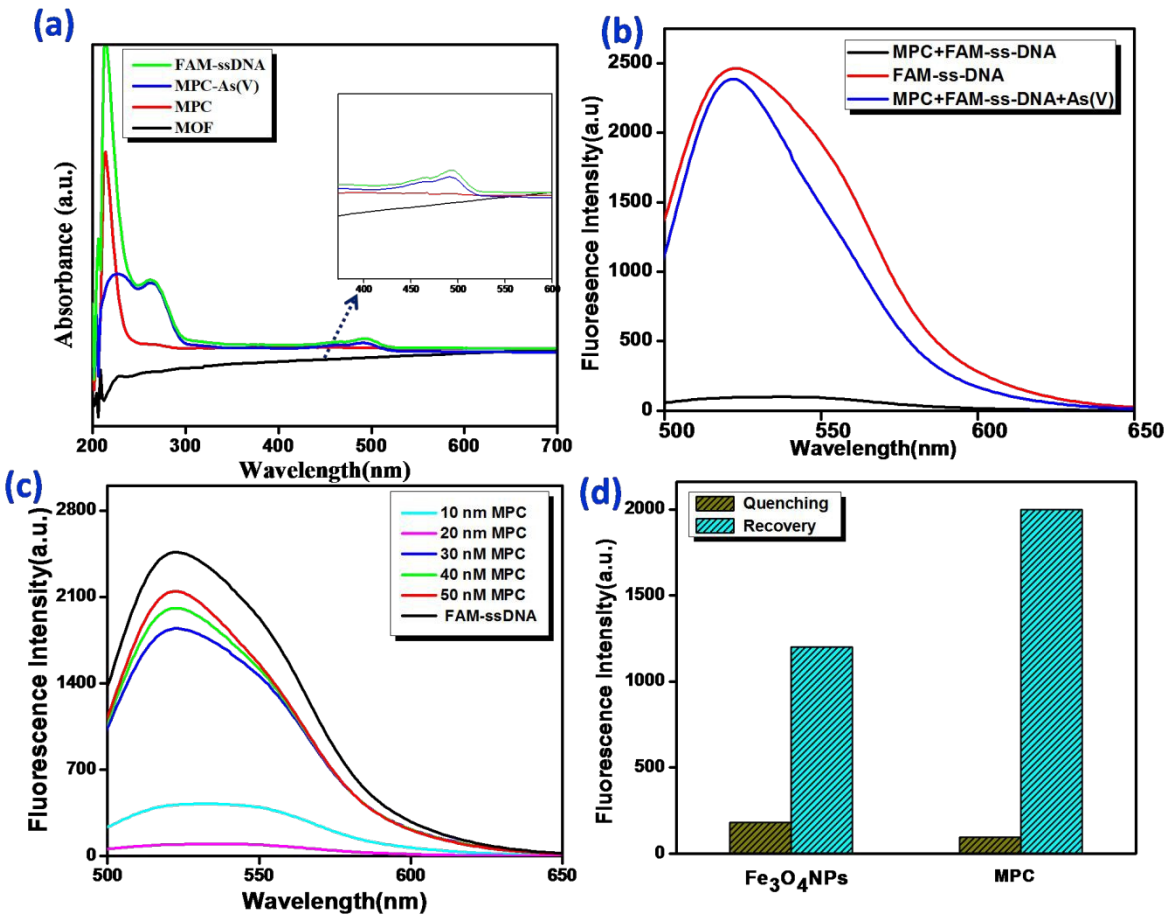

Fig.8.(a) UV-Visible spectra of MPC/FAM-ssDNA sense before and after addition As(V), (b) Fluorescence spectra of MPC/FAM-ssDNA explain quenching and recovery, (c) the optimization of different concentration of FAM-ssDNA into MPC composites, (d) comparison of Fe_3O_4 NPs and MPC composites.

3.4 Sensitivity and selectivity of arsenate (V)

The fluorescence responses of this sensing system to evaluate the various concentrations (0-15nm) of As (V) with addition of MPC composites and FAM-ssDNA. The mixing of MPC composites and FAM-ssDNA the formation of MPC / FAM-ssDNA showed at low fluorescence emission intensity. The fluorescence intensity dramatically enhanced with increasing the concentration of As (V) in the range from 0 to 15 nM. The relative fluorescence intensity and

View Article Online
DOI: 10.1039/C9AN00139E

concentration of arsenate (V) as displayed in Figure.5b. The linear relationship between the fluorescence intensity at 520 nm and the concentrations of As (V) in the range of 1-5 nM. The correlation coefficient value R^2= 0.976 (Fig.6d) with a detection limit of 630 pM was calculated from according to the 3σ method. In this study, exhibits very high sensitive detection of arsenate compared to other type of arsenate detection sensing system (Table 1), this may be due to metal-organic frameworks surface containing Fe_3O_4 NPs and carboxylic groups may be enhance the sensitivity of this sensing system.

In order to evaluate the selectivity of this sensor, it was investigated in the presence of potentially interfering with various anions and cations. In Figure 6d shows that the response of a fluorescence spectra to different ions including silver, arsenite, cadmium, mercury, bromide, sulfate, fluoride, phosphate and arsenate ions. The arsenate has been showing high fluorescence enhancement due to high affinity to the surface MPC composites [33]. The result showed that arsenate is highly selective in this sensing system compared to other anions and cations except phosphate. Phosphate also showed significant fluorescence intensity of this sensing system but binding affinity is very less compared to arsenate. Therefore, the proposed our sensing system is highly selectively detected for arsenate and no interference with other anions and cations.

View Article Online
DOI: 10.1039/C9AN00139E

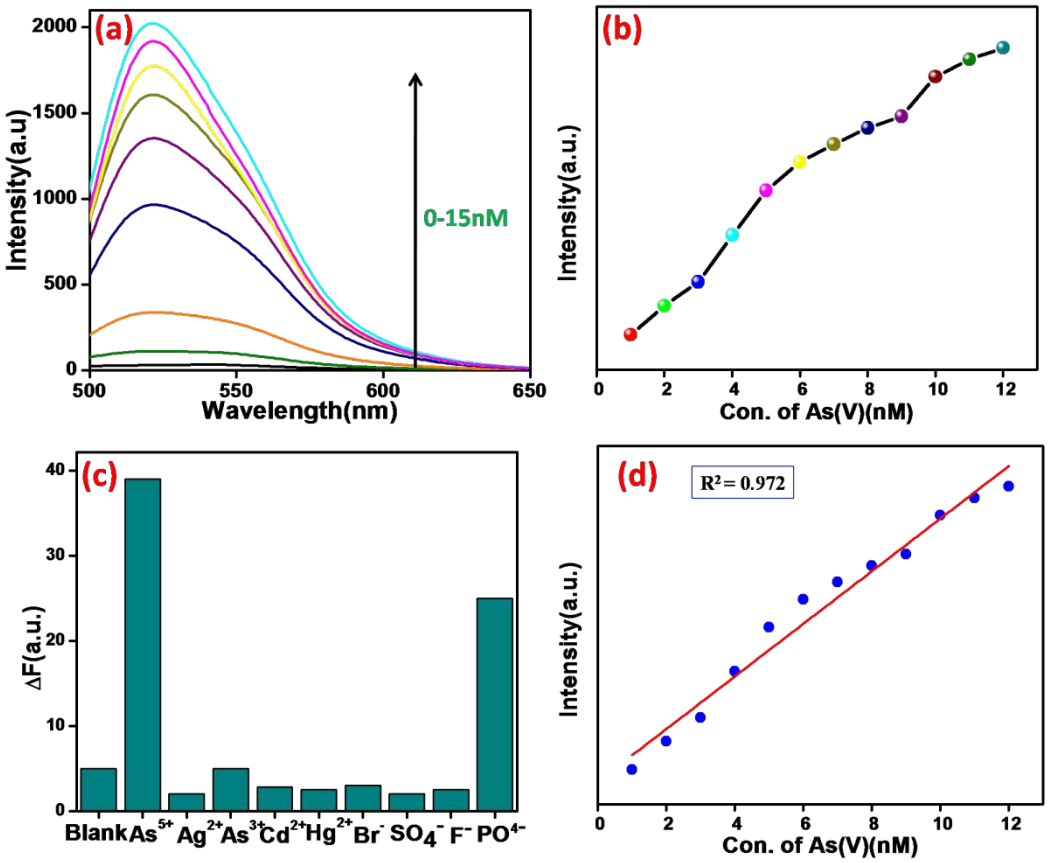

Fig.9. (a) Estimation with different concentration (0-15nm) of As(V),(b) the relative fluorescence intensity detection of As(V) based on MPC composites,(c) selectivity studies with other anions and cations,(d) Sensitivity of arsenate detection by this arsenate de-adsorption method.

View Article Online
DOI: 10.1039/C9AN00139E

Table.1 Comparison of detection of As (V) in another sensing system

Quenching Materials	**Method**	**LOD**	**Ref**
Modified gold nanoparticles(Au NPs)	Colorimetric	2.5 bbp	43
Gold nanoparticles(Au NPs)	Colorimetric	1 bbp	44
Polyhedral silver nanoparticles	Surface enhanced Raman scattering	1 bbp	45
Fe_3O_4 NPs	Fluorescence	300 nM	24
CeO_2	Fluorescence	29 nM	25
functionalized Merrifield polymer(APC)	Fluorescence	0.001 mM	46
Ruthenium bipyridine – graphene oxide nanocomposites	Electrochemical	43 nM	47
MPC composites	Fluorescence	630 pM	This work

View Article Online
DOI: 10.1039/C9AN00139E

4. CONCLUSION

In summary, a new As (V) probe was successfully designed, based on Metal-Organic framework derived magnetic porous carbon (MPC) composites. In this composites have been as superior quenching and magnetic properties owing to predominantly bind with FAM-ssDNA and As(V), especially in present sensing system working turn "off " and "On" sensor (adsorption and desorption) occurred in simultaneously. Under the optimized condition, the complex exhibit high selectivity and sensitivity for As (V) ion over other competitive metal ion. The detection limit of this sensor is as low as 630 pM, which so far below the maximum recommended limit in drinking water defined by the Environmental Protection Agency. Moreover, this sensing system compare to previous sensing assay to excellent selectivity and sensitivity of As (V) ion. We anticipate that this report of a fluorescent based biosensor for simplicity, higher stability and excellent analytical performance. In addition, the proposed MPC biosensor might be potentially can be applicable other environmental samples and biological applications from the scientific community.

Acknowledgements

In this study was supported by the Department of Chemistry and SRM-SCIF from SRM Institute of Science and Technology, Tamil Nadu - 603 203, India.

View Article Online
DOI: 10.1039/C9AN00139E

Reference

1. D. K. Nordstrom, *Science., 2002,* ***296****, 2143–2145.*
2. C. F. McGuigan, C. L. A. Hamula, S. Huang, S. Gabos and X. C. Le, *Environ. Rev., 2010,* ***18****, 291–307.*
3. Khan, N. A.; Hasan, Z.; Jhung, S. H, *J. Hazard. Mater., 2013,* ***245****, 444-56.*
4. Li, J. R.; Sculley, J.; Zhou, H. C. *Chem. Rev., 2012,* ***112****, 869-932.*
5. S. Shen, X.-F. Li, W.R. Cullen, M. Weinfeld, X.C. Le, *Chem. Rev., 2013,* ***113*** *, 7769–7792.*
6. M. Elias, A. Wellner, K. Goldin-Azulay, E. Chabriere, J.A. Vorholt, T.J. Erb, D.S.Tewfik, *Nature, 2012,* ***491****, 134–137.*
7. United States Environ. Prot. Agency. Arsen. Clarifications of compliance new source monit. Rule A Quick Ref. *Guide. EPA 816-F-01-004*
8. P. L. Smedley, D. G. Kinniburg, *Appl.Geo.chem., 2002,****17****,517-568.*
9. Yuangen Wu, Shenshan Zhan, Haibo Xing, Lan He, Lurong Xu and Pei Zhou, *Nanoscale, 2012,* ***4****, 00–00.*
10. Shenshan Zhan, Minglei Yu, Jing Lv,Lumei Wang, and Pei Zhou, *Aust. J. Chem. 2014,* ***67****, 813–818.*
11. Yuangen Wu,aFaze Wang, Shenshan Zhan, Le Liu,a Yanfang Luo and Pei Zhou, *RSC Adv., 2013,* ***3,*** *25614–25619.*
12. Lulu Song, KangMao, XiaodongZhou, JimingHu, Talanta.,2016,146, 285–290
13. M. Colon, M. Hidalgo, M. Lglesias, *Talanta.,2011,* ***85****, 1941-1947.*
14. E. H. Larsen and S. Sturup, J. Anal, *At. Spectrom., 1994,* ***9****, 1099–1105.*
15. M. Mulvihill, A. Tao, K. Benjauthrit, J. Arnold and P. Yang, *Angew.Chem., Int. Ed., 2008,* ***47****, 6456–6460.*

View Article Online
DOI: 10.1039/C9AN00139E

16. J. Li, L. Chen, T. Lou and Y. Wang, *ACS Appl. Mater. Interfaces, 2011, **3**, 3936–3941*.

17. Y. Zhou, X. Huang, C. Liu, R. Zhang, X. Gu, G. Guan, C. Jiang, L. Zhang, S. Du, B. Liu, M.-Y. Han and Z. Zhang, *Anal. Chem., 2016, **88**, 6105-6109.*

18. Ravikumar, A.; Panneerselvam, P.; Radhakrishnan, K, *Microchim Acta., 2018, **2**, 182*.

19. Saran, R.; Liu, J, *Anal. Chem., 2016, **887**, 4014-4020*.

20. Zhang, S. Zhang, D. Zhnag, X. Shang, D. Xue, Z. Shan, D. Quan Lu, X, *Anal. Chem., 2017, **89**, 3538-3544*.

21. Li. B.; Du, Y.; Dong. S,*Anal. Chim. Acta., 2009, **644**, 78-82*.

22. Zhang, Y.; Zeng, G. M.; Tang, L.; Li, Y. P.; Chen, Z. M.; Huang, G. H. *RSC. Adv., 2014, 18485 -18492*

23. S. Laurent, D. Forge, M. Port, A.Roch,C. Robic, L. Vander Elst, and R. N. Muller *,Chem. Rev., 2008, **108**, 2064–211.*

24. Biwu Liu and Juewen Liu, *Chem. Commun., 2014, **50**, 8568-8570*

25. Anand Lopez, Yifei Zhang, Juewen Liu. *J. Colloid. Interface Sci., 2017, **493**,249-256.*

26. A. Anand Babu Christus, P. Panneerselvam, A. Ravikumar, *Anal. Methods**, 2018**, 10,** 4378-4386* .

27. J. R. Li, R. J. Kpleraup, H. C. Zhou, *Chem. Soc. Rev., 2009, **38**, 1477.*

28. J. Y. Lee, O. K.Farha, J. Roberts, K. A. Scheidt, S. T. Nguyena, J. T. Hupp, *Chem. Soc. Rev., 2009, **38**, 1450.*

29. P. Karthik, R. Vinoth, P. Zhang, W. Choi, E. Balaraman and B Neppolian., *ACS Appl. Energy Mater.*,2018, **1** ,5, 1913–1923.

30. Das, R., Pachfule, P., Banerjee, R. & Poddar, P, *Nanoscale., 2012, **4,** 591–599.*

31. Zhang, L., Wu, H. B. & Lou, *J. Am. Chem. Soc., 2013, **135**, 10664-10672*

View Article Online
DOI: 10.1039/C9AN00139E

32. P. Karthik ,A. Pandikumar,M. Preeyanghaa,M. Kowsalya, B.Neppolian., *Microchim Acta 2017 ,**184**,2265–2273.*

33. X. Zhu, H. Zheng, X. Wei, Z. Lin, L. Guo, B. Qiu, G., *Com-mun.,2013,**49,** 1276-1278.*

34. H.-T. Zhang, J.-W. Zhang, G. Huang, Z.-Y. Du, H.-L. Jiang, *Chem. Commun., 2014, **50,** 12069-12072.*

35. L.L. Wu, Z. Wang, S.N. Zhao, X. Meng, X.Z. Song, J. Feng, S.Y. Song, and H. J. Zhang, *Chem. Eur. J., 2016, **22**, 477-480.*

36. J. Tian, Q. Liu, J. Shi, J. Hu, A.M. Asiri, X. Sun, Y. He, *Biosens. Bio- electron., 2015, **71,**1-6.*

37. P. Horcajada1, T. Chalati, C. Serre, B. Gillet, C. Sebrie, T. Baati, J. F.Eubank, D. Heurtaux, P. Clayette, C. Kreuz, J. Chang, Y. K. Hwang,V. Marsaud, P. Bories, L. Cynober, S. Gil, G. Férey, P. Couvreur and R. Gref, *Nat. Mater*., 2010, **9**, 172.

38. Ayyanu Ravikumar, Perumal Panneerselvam, and Norhashimah Morad ACS *Appl. Mater. Interfaces*., *2018,10,20550-20558.*

39. Hongliang Tan, Gonge Tang, Zhixiong Wang, Qian Li, Jie Gao, Shimeng Wu, *Anal. Chim. Acta., 2016, **940**, 136-142.*

40. Kim, J.S. and Quang D.T, *Chem. Rev.,* 2007, *107, 3780*-3799.

41. Ni, X.L., Chen, S., Yang, Y. and Tao, Z., *J. Am. Chem. Soc.,* 2016, 138, 6177-6183.

42. Gui, B., Meng, Y., Xie, Y., Tian, J., Yu, G., Zeng, W., Zhang, G., Gong, S., Yang, C., Zhang, D. and Wang, C., *Advanced Materials, 2018, 3, 1802329*.

43. F. Liu, A. De Cristofaro and A. Violante, *Soil Sci., 2001, **166**, 197–208.*

44. R. D.Gonzalez, L. G. Varela and P. B.Barrera, *Talanta, 2014, **118,** 262–269.*

View Article Online
DOI: 10.1039/C9AN00139E

45. J. R. Kalluri, T. Arbneshi, S. Afrin Khan, A. Neely, P. Candice, B. Varisli, M. Washington, S. McAfee, B. Robinson, S. Banerjee, A. K. Singh, D. Senapati and P. C. Ray*, Angew. Chem., Int. Ed., 2009, **48**, 9668–9671.*

46. M. Mulvihill, A. Tao, K. Benjauthrit, J. Arnold and P. Yang, *Angew.Chem .Int. Ed., 2008, **47**, 6456–6460.*

47. Ziping Liu, Guodong Li, Tingting Xia, Xingguang Su, *Sensors and Actuators B: Chemical., 2015, **220**, 1205-1211*.

View Article Online
DOI: 10.1039/C9AN00139E

TOC: